

# Laser Surface Engineering of Nylon 6.6 and the Effects Thereof on Adhesion and Biomimetic Apatite Coating Formation

**David Waugh and Jonathan Lawrence**

Accepted manuscript PDF deposited in Coventry University's Repository

**Original citation:**

Waugh, D. G., and J. Lawrence. "Laser Surface Engineering of Nylon 6.6 and the Effects Thereof on Adhesion and Biomimetic Apatite Coating Formation." *Lasers in Engineering*, 39 (2018).

<http://www.oldcitypublishing.com/wp-content/uploads/2018/09/LIEv39n1-2p77-95Waugh.pdf>

ISSN: 0898-1507

Publisher: Old City Publishing

**Copyright © and Moral Rights are retained by the author(s) and/ or other copyright owners. A copy can be downloaded for personal non-commercial research or study, without prior permission or charge. This item cannot be reproduced or quoted extensively from without first obtaining permission in writing from the copyright holder(s). The content must not be changed in any way or sold commercially in any format or medium without the formal permission of the copyright holders.**

# LASER SURFACE TREATMENTS AND THEIR EFFECTS ON ADHESION AND BIOMIMETIC APATITE COATING FORMATION

Paper #M201

D.G. Waugh, J. Lawrence

Laser Engineering and Manufacturing Research Centre, University of Chester, Parkgate Road, Chester CH1 4BJ, UK

## Abstract

Within the field of bioengineering, simulated body fluid (SBF) has been widely implemented as a technique to screen for the bioactivity of materials. Furthermore, SBF can be used in the biological industry to promote the adhesion of apatite coatings to assist with making materials more biomimetic. This paper details the use of CO<sub>2</sub> and KrF excimer lasers for the surface treatment of nylon 6,6 to modulate apatite formation following immersion in SBF for 14 days. Following CO<sub>2</sub> laser surface treatment, using white light interferometry, the surface roughness increased to a maximum of R<sub>a</sub> and S<sub>a</sub> of 1.3 and 4.4 μm, respectively. X-ray photoelectron spectroscopy (XPS) analysis showed a maximum increase in surface oxygen content of 5.6 %at. CO<sub>2</sub> laser-induced surface modifications gave rise to a modulation in the wettability characteristics such that the contact angle,  $\theta$ , decreased for the whole area processed samples, as expected, and increased for the patterned samples. For the KrF excimer laser processed samples, it was found that S<sub>a</sub> increased by up to 1.5 μm when compared to the as-received sample. After 14 days of immersion in SBF each sample was analysed using SEM and EDX to ascertain the presence of apatite crystals formed on the as-received and laser treated nylon 6,6 surfaces. It was seen for all samples that calcium phosphate formed on each surface following 14 days. An increase in mass for the laser processed samples indicated that these modified surfaces gave rise to an accelerated formation of apatite when compared to the as-received sample. This, along with strong correlations between  $\theta$ , the surface energy parameters and the calcium phosphate formation, for whole area processed samples, highlights the potential for this surface treatment technique for predicting and enhancing the bone forming ability of laser processed materials.

## Introduction

To determine the bioactivity and biofunctionality of materials, simulated body fluid (SBF), which is a metastable calcium phosphate solution, has been extensively implemented within the bioengineering

industry [1, 2]. The increased use of SBF within this field is a result of the fact that, for almost all orthopaedic materials, there is a strong, correlative link between the ability to form bone-like carbonate apatite crystals and the osseointegration potential of that material [2-4]. Furthermore, this very important apatite crystal layer is associated with specific bone proteins that are significant for bone reconstruction [5].

Various materials such as metals, ceramics and polymers have been used for biomedical applications [6-10]. Nylon is a low cost, semi-crystalline thermoplastic and has been used for such biological applications as sutures, vascular grafts and other hard tissue implants [11]. Although there is an increased focus on polymers by industry on account of their relative inexpensive cost and ease of manufacturing manipulation, many polymers do not possess sufficient surface properties to give rise to adequate osseointegration [9, 12]. This can lead to discomfort to the patient, increased need for corrective surgery and an increase in the economic costs involved. Through surface modification of polymeric materials it is believed that their surfaces can be enhanced to lend them to more biological applications [9, 12-14].

Laser surface engineering holds a number of benefits over competing techniques [7] such as it can be accurate, precise, flexible and non-contact. In addition, lasers enable one to have the ability to modify both the surface topography and surface chemistry, keeping the bulk material unchanged. The modification of both the surface chemistry and topography on micro- and nano-scales can also be seen to lend itself to have a major impact on the material wettability characteristics [15-17]. Furthermore, lasers also offer the opportunity of inducing varying and predictable levels of topography/roughness depending on how the laser is employed. For instance, periodic patterns can be induced using a focused beam [18, 19] whereas a more random pattern can be employed using a larger, more divergent, laser beam [20, 21].

There is an increasing demand for biological implants and biological therapies [22] on account of an ageing

worldwide population. On account of this, it is of critical importance for the bioengineering industry to devise and implement a cost-effective and practically efficient method to manufacture cheap implants and platforms upon which to grow various cell lines such as mesenchymal stem cells. Surface treatment techniques currently available within the bio-technology industry for surface modification are somewhat limited and expensive, involving numerous processing steps [9, 23-25]. This will have a major impact upon the industry insofar as it will hinder expansion and seriously limit the applications for polymers due to insufficient surface properties. Previous work has shown that these laser-induced surface modifications have a relationship with the wettability characteristics for polymers [12, 26, 27]. Furthermore, it has been evidenced that there is a relationship between the wettability characteristics and bioactive nature of the nylon 6,6 in terms of osteoblast cell growth [12, 26, 28].

On account of the importance and great need for more efficient polymeric biomaterials, this work details the flexible use of two different lasers (CO<sub>2</sub> laser and KrF laser) for surface engineering of nylon 6,6. The effects on surface topography, surface chemistry and wettability/adhesion are discussed. In addition, the implementation of the SBF screening method is discussed to show that laser surface engineering can be implemented to modulate the biofunctionality of nylon 6,6 and is a technique which can be readily applied to polymeric materials to meet the needs and demands of the bioengineering industry.

## **Experimental Technique**

### **Materials**

The nylon 6,6 material was used in 100×100 mm<sup>2</sup> sheets and had a thickness of 3mm (Goodfellow Cambridge, Ltd.). To obtain conveniently sized samples a continuous wave (cw) 1 kW CO<sub>2</sub> laser (Everlase S48; Coherent, Ltd.) was employed to cut the sheets into circular samples with diameters of 25 mm.

### **Laser Surface Engineering**

#### CO<sub>2</sub> Laser Surface Engineering

In order to generate the required marking pattern with the 10 W CO<sub>2</sub> laser system (10 W; Synrad, Inc.), Synrad Winmark software version 2.1.0, build 3468 was used. Further details of the CO<sub>2</sub> laser set-up is provided in [21].

For the CO<sub>2</sub> laser surface patterned samples, four patterns were induced onto the surfaces of the nylon 6,6 samples; these were 50 µm spaced trenches (CT50), 50

µm spaced hatch (CH50), 100 µm spaced trenches (CT50) and 100 µm spaced hatch (CH100). For the CO<sub>2</sub> laser surface patterning the laser power was set constant to 70% (7 W) with a constant scan speed of 600 mms<sup>-1</sup>.

For relative large area processing, a cw 100 W CO<sub>2</sub> laser (DLC; Spectron, Ltd) was used to scan a 5mm diameter beam across the target sample with one pass in order to irradiate the test area with an irradiance of 510 Wcm<sup>-2</sup>. Scanning speeds of 150, 100, 75, 50, 25 and 20 mms<sup>-1</sup> were used to irradiate six samples with effective fluences of 16.84 (samples CWA17), 25.51 (sample CWA26), 34.18 (sample CWA34), 51.02 (sample CWA51), 102.04 (sample CWA102) and 127.55 (sample CWA128) Jcm<sup>-2</sup>, respectively.

#### KrF Laser Surface Engineering

A 248 nm KrF excimer laser (LPX 200i; Lambda Physik, Inc.), using two different setups, were implemented to carry out the patterned and large area processing.

For the patterned experiments the repetition rate was kept constant at 25 Hz, with a number of 10 pulses per site and used Aerotech CNC programming to induce the required pattern. The patterns induced using this technique were 50 µm trench (T50), 100 µm trench (T100), 50 µm hatch (H50) and 100 µm (H100).

For the large area processing the raw 23 × 12 mm<sup>2</sup> beam was used to irradiate a large section of each sample at a time. For the large area processing experiments 6 samples were irradiated; these being 100 pulses at 100 mJ (WA100), 100 pulses at 150 mJ (WA150), 100 pulses at 200 mJ (WA200), 100 pulses at 250 mJ (WA250), 500 pulses at 250 mJ (WA250\_500) and 1000 pulses at 250 mJ (WA250\_1000). This gave fluences of 36±3, 54±5, 72±8 and 91±10 mJcm<sup>-2</sup>, respectively for the different energies used. Throughout the large area KrF excimer laser experiments the repetition rate was kept constant at 25 Hz and Aerotech CNC programming ensured that the correct number of pulses was applied to each sample. Further details of the KrF excimer laser set-up is provided in [20].

#### **Analytical Techniques**

Ultrasonic cleaning in isopropanol (Fisher Scientific Ltd., UK) for 3 minutes was carried out to remove any debris which may have formed during the laser processing. Surface profiles were determined using a white light interferometer (WLI) (NewView 500; Zygo, Ltd) with MetroPro and TalyMap Gold Software. Further details of the surface profiling is provided in [21].

In accordance with Rance [29] the samples were analysed using a goniometer (OCA20; Dataphysics Instruments, GmbH) to determine various wettability characteristics. Further details of the contact angle measurements are given in [28]. In addition, all samples were analysed using x-ray photoelectron spectroscopy (XPS) analysis. This allowed any surface modifications in terms of surface oxygen content due to the laser irradiation to be revealed. Further details of the XPS analysis is given in [20].

### Apatite Coating Formation and Analysis

The SBF protocol was implemented in accordance with [20]. Prior to using the SBF all of the samples and apparatus to be used were autoclaved. The samples were then placed into sterile 30 ml glass containers, immersed in 30 ml of SBF and placed into an incubator to keep the temperature constant at 37 °C for 14 days.

Prior to the implementation of the SBF screening protocol, the nylon 6,6 samples were weighed using a balance (S-403; Denver Instrument, GmbH) with a readability of 0.001g. The samples were weighed, fully dry, before and after the SBF immersion in order to ascertain the weight difference before and after the experimentation. Following this, samples were gold coated and analysed using scanning electron microscopy (SEM). Furthermore, the samples were analysed using energy dispersive x-ray (EDX).

## Results and Discussion

### Effects of Laser Surface Engineering on Topography

As expected, using a CO<sub>2</sub> laser to scan a predetermined pattern across the nylon 6,6 surfaces elicited a significant variation in topography when compared to the as-received sample (AR). This is more apparent when comparing the 3-D profiles and profile extractions of the as-received sample (see Figure 1) and the laser patterned samples (see Figure 2).

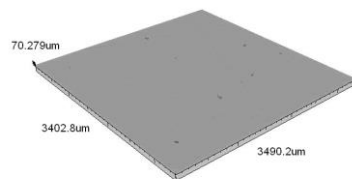
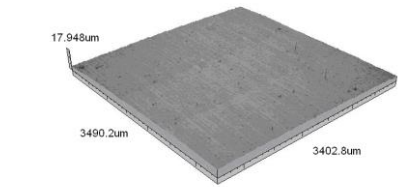


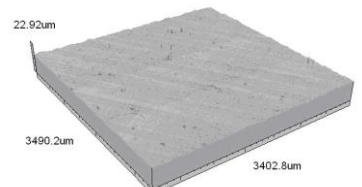
Figure 1 – Continuous axonometric 3-D image and profile extraction for the as-received sample (AR).

Comparing Figure 1 and Figure 2 the CO<sub>2</sub> laser-patterned samples had rougher surfaces with maximum

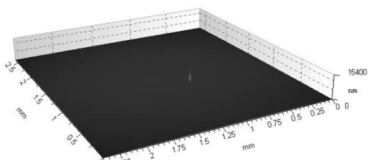
peak heights around 2 µm. As a result of this, the surface roughness (see Figure 3) increased considerably with the largest Sa of 0.4 µm being achieved with sample CH50. Samples CT50 and CH50 had greater Sa roughness values when compared to CT100 and CH100 on account of the 50 µm scan patterns irradiating a larger area, increasing the amount of material undergoing melting and re-solidification. Figure 2 also allows one to see that there was further evidence of considerable melting on account of one being able to identify craters left from evolved gases breaking at the surface. This is especially apparent for sample CWA102 and sample CWA128.



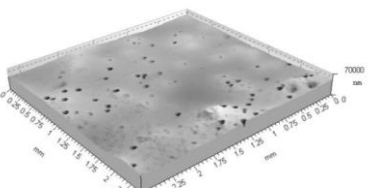
(a)



(b)



(c)



(d)

Figure 2: 3-D images for selected samples (a) CT50 (b) CH100 (c) CWA17 and (d) CWA128.

With regards to the scanned pattern, sample CT50 and sample CH50 gave rise to the smallest periodicity. This can be accounted for by overlapping of the scanned pattern due to the laser beam spot size, incident on the surface, being approximately 95 µm. This also provides

an explanation as to why the Sa increased as for samples CT50 and CH50, which had up to a three times larger Sa values compared to the other CO<sub>2</sub> laser surface engineered samples. The CO<sub>2</sub> laser whole area surface engineering of the nylon 6,6 elicited a significantly modified surface, especially for sample CWA102 and CWA128, which had considerably higher fluences incident on the surface.

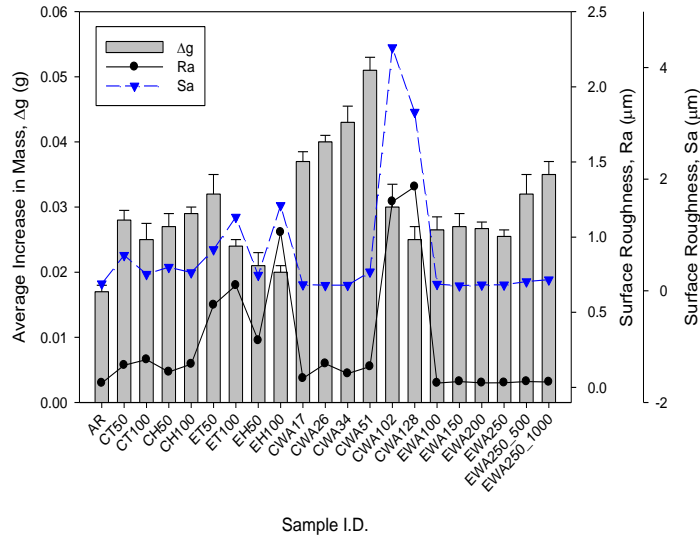


Figure 3: Graph showing average increase in mass following immersion in SBF and the surface roughness for each sample.

Through excimer laser patterning (see Figure 4(a) and 4(b)) the surface of the nylon 6,6 had been greatly modified. Trench depths of between 1 μm and 5 μm was observed for the laser set-up which was implemented. For the excimer laser large area surface engineered samples (see Figure 4(c) and 4(d)), they had a similar topography to that of the as-received sample (see Figure 1). With this in mind, it is likely that the nylon 6,6 material did not ablate due to the threshold fluence not being surpassed [30].

Comparing the two laser processed used within this work, the result show that the excimer laser surface engineering (see Figure 3) gave rise to a more accurate and repeatable means of modifying the topography and roughness of the nylon 6,6 samples. This is due to the wavelength of the two lasers giving rise to different laser-material interactions [31].

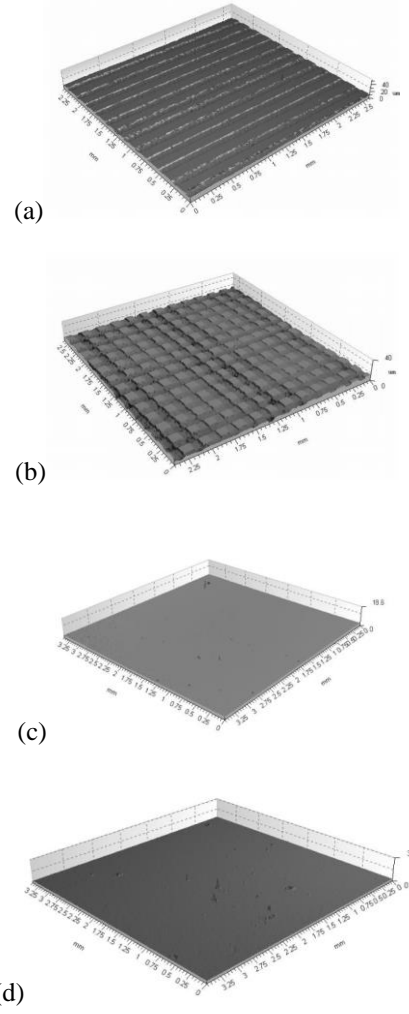


Figure 4: 3-D images for selected samples (a) ET100 (b) EH100 (c) EWA100 and (d) EWA250\_1000.

### Effects of Laser Surface Engineering on Surface Chemistry and Wettability Characteristics

For a hydrophilic material such as nylon 6,6 an increase in roughness and surface oxygen content should bring about a reduction in  $\theta$  [32, 33]. Having said that, the data obtained and shown in Figure 3 and Figure 5 indicate that the CO<sub>2</sub> laser surface-patterned samples gave rise to an increase in contact angle,  $\theta$ , of up to 10°. It was also observed for the KrF excimer laser surface-patterned samples which gave rise to an increase in  $\theta$  of up to 24°. This phenomenon can be explained by the existence of a mixed-state wetting regime [27, 34] in which both Cassie-Baxter and Wenzel regimes coexist. This mixed-state wetting regime can also account for the observed reduction in polar component,  $\gamma^p$ , and total surface-free energy  $\gamma^T$  (see Figure 5(b)).

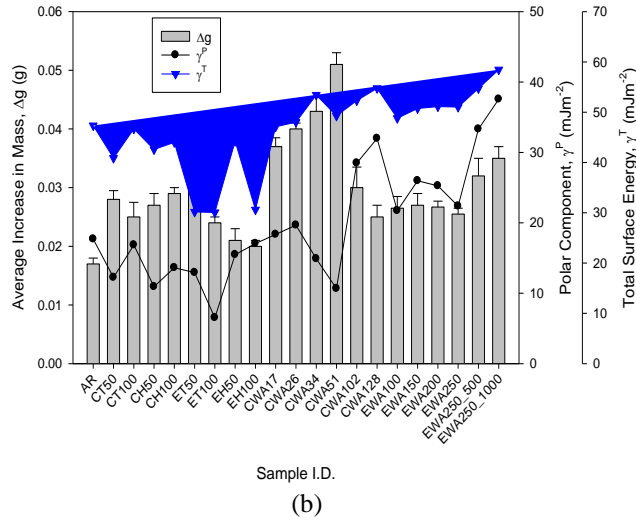
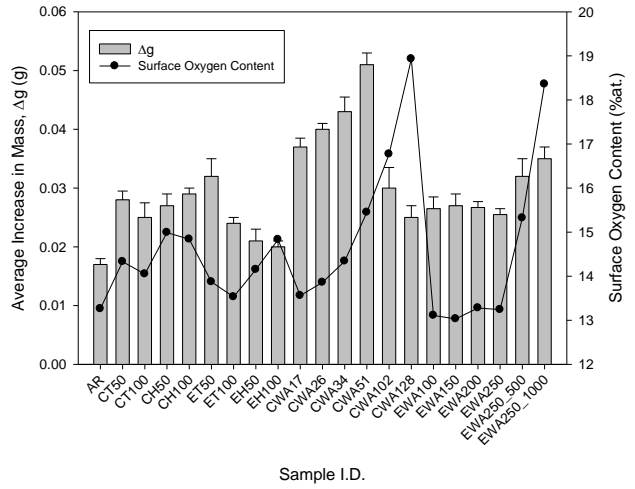
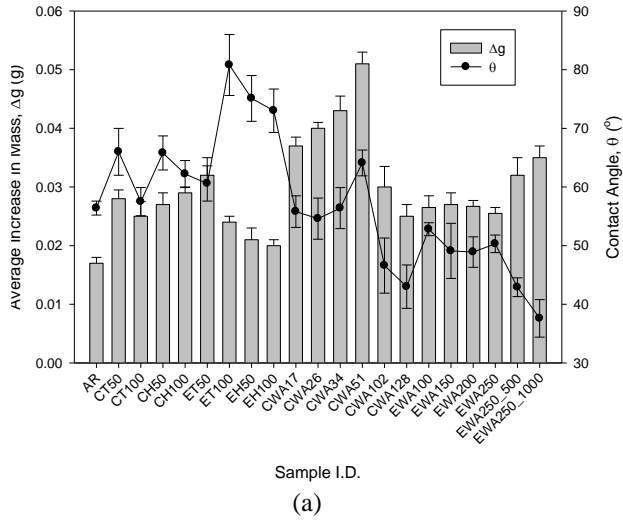


Figure 5: Graph showing average increase in mass following immersion in SBF and the surface energy parameters for each sample.

As shown in Figure 5, both the CO<sub>2</sub> and excimer laser whole area surface engineered samples gave rise to a reduction in  $\theta$  of up to 20° compared to the as-received sample. This corresponded with current theory such that the reduction in  $\theta$  arose from the increased surface roughness.

Figure 6 gives the surface oxygen content for all samples and it was observed that for most of the laser surface engineered samples the surface oxygen content increased by up to 5% at. when compared to the as-received sample (AR). This slight modification with a small increase in surface oxygen indicates that the significant variation in nylon 6,6 surface topography brought about the distinct change in wettability.

Figure 6: Graph showing average increase in mass following immersion in SBF and the surface oxygen content for each sample.

### Effects of Laser Surface Engineering on Apatite Coating Formation

Following immersion in SBF only a very small amount of sediment was present on the as-received sample (see Figure 7) in comparison to the laser surface engineered samples (see Figure 8 and Figure 9). Through CO<sub>2</sub> laser surface engineering (see Figures 8(a) and (b)) it was observed that the apatite sediment preferentially formed around craters that were formed on account of evolved gases breaking at the surface during the laser-induced melting. In a similar fashion (see Figure 9), it was observed for the excimer laser patterned samples that the apatite preferentially formed around the ablated tracks induced in to the nylon 6,6 material. This is significant as it indicates that these types of laser processing could give rise to cell growth directionality and provide a means to achieve areas on the surface of polymeric materials for preferential biological cell growth.

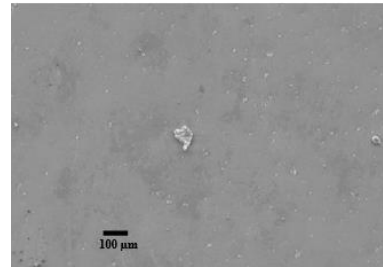


Figure 7: SEM micrograph of the as-received sample following immersion in SBF.

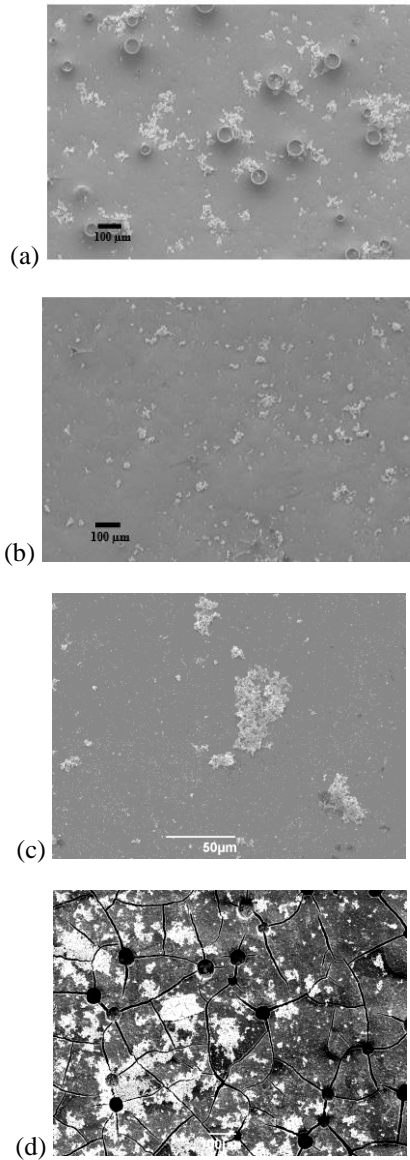


Figure 8: SEM micrographs of sample (a) CT50, (b) CH50, (c) CWA26 and (d) CWA128 following immersion in SBF.

It is also significant to note that all laser surface engineered samples gave rise to an increase in mass,  $\Delta g$  (see Figure 6). This can be accounted for by the increase in apatite formation on the sample surfaces. Samples CT50, CT100, CH50 and CH100 gave rise to a larger increase mass when compared to the as-received sample (AR) and the excimer laser processed samples by up to 0.015 g. For the CO<sub>2</sub> laser whole area processed samples  $\Delta g$  increased considerably when compared to the as-received sample (AR). The increase in  $\Delta g$  for the CO<sub>2</sub> laser whole area processed samples had increased by at most 0.05 g. In comparison to the excimer laser whole area processed samples the CO<sub>2</sub> laser gave rise to a

larger increase in apatite formation. Having said that, the excimer laser whole area processed samples gave rise to an increase in  $\Delta g$  of up to 0.02 g compared to the as-received sample. Another factor which can be taken from Figure 6 is that the increase in mass steadily increased from sample CWA17 to sample CWA51 which gave the largest increase in mass of 0.05 g. This suggests an operating window of between 17 Jcm<sup>-2</sup> and 51 Jcm<sup>-2</sup> to achieve the optimum surface to promote apatite formation.

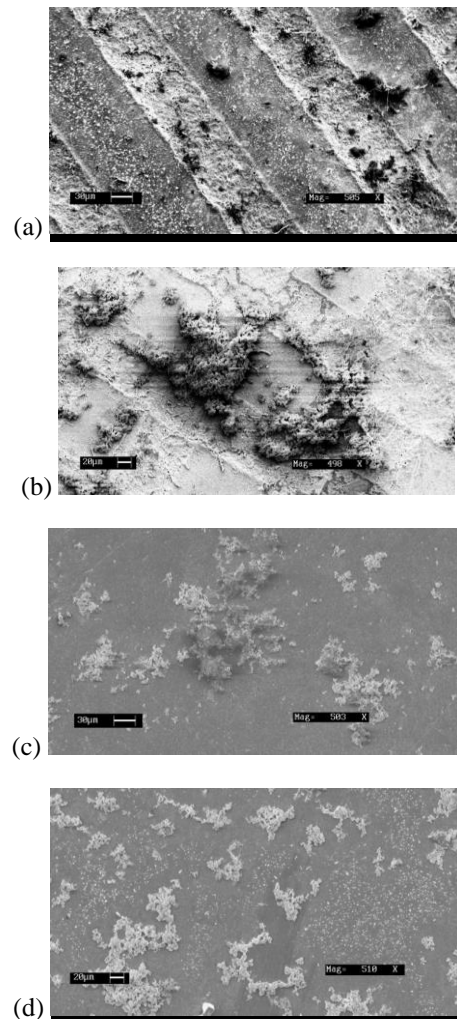


Figure 9: SEM micrographs of sample (a) ET100, (b) EH100, (c) EWA250\_500 and (d) EWA250\_1000 following immersion in SBF.

In order to confirm the existence of apatite on the surface of the samples studied, Figure 10 shows the surface elemental data for the as-received sample (AR) and a typical CO<sub>2</sub> laser surface modified nylon 6,6 sample, indicating that both phosphorous and calcium were present, following the formation of the calcium phosphate apatite. This is of importance due to

phosphorous and calcium having to be present to inherently increase the biomimetic nature of the material in terms of the bone-bonding and osseointegration ability.

Figure 5(a) shows the increase in mass for each sample in relation to the laser-modified  $\theta$ . As the mass increase for the excimer laser processed samples was small any relationships between the surface properties and  $\Delta g$  was difficult to ascertain. It was also found that for the CO<sub>2</sub> laser-induced patterned nylon 6,6 samples was no correlation between the level of apatite formation and the laser-modified  $\theta$ . This could be owed to the transition in wetting regime playing a significant role in the biomimetic nature of the nylon 6,6 samples. The CO<sub>2</sub> laser whole area laser processed sample, on the other hand, did show a relationship between  $\Delta g$  and the laser-modified contact angle. That is, for samples CWA17, CWA26, CWA34 and CWA51 the increase in laser-modified  $\theta$  elicited an increase in  $\Delta g$ . Then for samples CWA102 and CWA128, with an increase in fluence,  $\theta$  decreased leading to an increase in  $\Delta g$ . This could be due to the material becoming too hydrophilic, hindering the initial protein adsorption required [12].

From Figure 5(b) it was determined that there was no correlative relationship between  $\Delta g$  for the CO<sub>2</sub> laser patterned samples and  $\gamma^p$  which can be attributed to the transitions in wetting regime. This was also the case for the excimer laser patterned samples. For both the CO<sub>2</sub> and excimer laser whole area processed samples it was observed that an increase in  $\gamma^p$ , an increase in  $\gamma^T$  and an increase in surface in oxygen content (see Figure 6) results in the nylon 6,6 to become more hydrophilic. As a result, this appears to have had a significant positive impact upon the formation of apatite when the samples were immersed in SBF.

Upon collating all of the contact angle, surface-free energy and increase in mass data for all laser surface engineered samples (see Figure 11), it was possible to consider the overall relationship between the laser-modified surface properties studied and the apatite formation. With the exception of the CO<sub>2</sub> laser whole area processed nylon 6,6 samples, Figure 11(a) shows that the mass increase,  $\Delta g$ , decreased on account of the laser-modified  $\theta$  increasing. In a similar fashion,  $\Delta g$  was an increasing function of the surface-free energy components,  $\gamma^p$  (see Figure 11(b)) and  $\gamma^T$  (see Figure 11(c)). It should be noted though, that the KrF excimer laser processed samples appeared to follow these trends more than the CO<sub>2</sub> laser surface engineered samples. This suggests that the dominant parameters to determine apatite adhesion could be very much dependent on the wavelength employed. This stands to reason as it is the laser wavelength which determines the laser-material

interaction and would likely elicit different material surface changes.

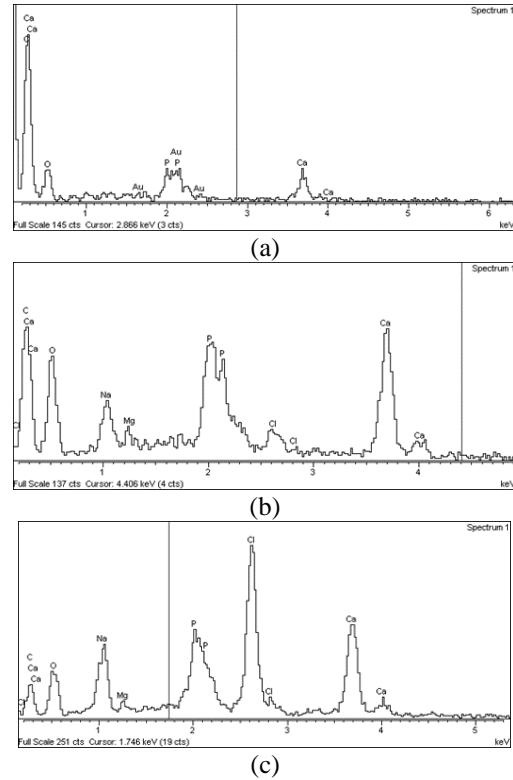


Figure 10: EDX spectra of (a) the as-received sample (AR) and (b) a typical CO<sub>2</sub> laser surface modified sample and (c) a typical KrF Excimer laser surface engineered sample following immersion in SBF after 14 days.

Finally, it should be noted that overall there was no observed correlation between  $\Delta g$  and the surface roughness and  $\Delta g$  and the surface chemistry. This could imply that wetting transitions play a major role in the adhesion of apatite to the surface of laser surface engineered nylon 6,6.

By taking into account all of the parameters it can be seen that for the majority of laser surface engineered nylon 6,6  $\theta$  and the surface-free energy components have the potential to be implemented as an indicative tool to allow one to estimate the apatite response of a laser-modified polymeric material. On the other hand, owed to the likely transition in wetting regime proposed having a great effect on the adhesion properties for the laser-induced patterned samples it should be noted that further work in this area is required to confirm the potential trends identified within this work.



## Conclusions

By implementing two different laser types for discrete patterning and large area processing it has been shown that laser surface engineering has the ability to modify the surface topography, surface chemistry and the wettability/adhesion characteristics of nylon 6,6. What is more, it has been shown that these laser-induced surface modifications can optimize the surface to provide a more efficient platform to promote the formation of apatite, enhancing the biomimetic nature of the nylon 6,6.

For the laser patterned samples (CO<sub>2</sub> laser and excimer laser) the contact angle,  $\theta$ , increased by up to 24° when compared to the as-received sample. In contrast, the large area laser processed samples gave rise to  $\theta$  either equivalent to the as-received sample or less by up to 20°. For the laser patterned samples, the observed increase in  $\theta$  is owed to the decrease in surface-free energy components on account of a transition in wetting regime to a mixed state. For all samples it the laser surface engineering elicited a positive response with regards to apatite formation in that more apatite preferentially formed on the laser engineered samples compared to the as-received sample. It should be noted that the largest increase in mass,  $\Delta g$ , owed to the apatite formation was found on the CO<sub>2</sub> laser whole area processed samples up to an incident fluence of 51 Jcm<sup>-2</sup>. It is believed that beyond this fluence the nylon 6,6 surface became too hydrophilic giving rise to apatite formation results similar to that of the other samples. Having said that, it was found that all laser surface engineered surfaces had an enhanced biofunctionality compared to the as-received sample.

The results within this study show how a polymeric material can be modified to become more biomimetic. With this in mind, laser surface engineering can be seen as a strong candidate to provide the bioengineering industry with a technique to meet the increasing socio-economic demands of an ageing worldwide population.

## References

- [1] Roach, P., Eglin, D., Rohde, K., Perry, C.C. (2007) Modern biomaterials: a review - bulk properties and implications of surface modifications. *Journal of Materials Science: Materials in Medicine* 18 1263-1277.
- [2] Song, W.H., Jun, Y.K., Han, Y., Hong, S.H. (2004) Biomimetic apatite coatings on micro-arc oxidized titania. *Biomaterials* 25 3341-3349.
- [3] Nagano, M., Kitsugi, T., Nakamura, T., Kokubo, T., Tanahashi, M. (1996) Bone bonding ability of an apatite-coated polymer produced using a biomimetic

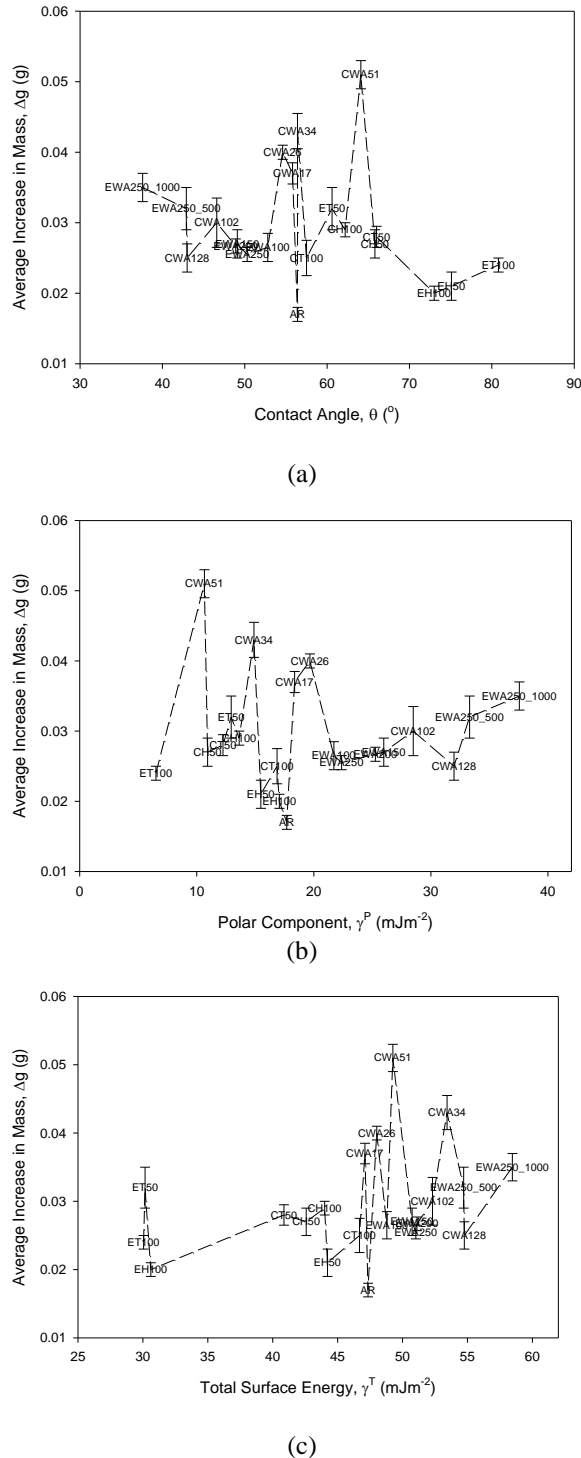


Figure 11: Graphs showing the relationship between  $\Delta g$  and (a) the contact angle, (b) the polar component and (c) the total surface-free energy.

- method: a mechanical and histological study in vivo. *Journal of Biomedical Materials Research*. 31 487-494.
- [4] Hao, L., Lawrence, J., Li, L. (2005) The wettability modification of bio-grade stainless steel in contact with simulated physiological liquids by the means of laser irradiation. *Applied Surface Science* 247 453-457.
- [5] Rey, C. (1998) Orthopedic biomaterials, bioactivity, biodegradation; a physical-chemical approach. *Journal of Biomechanics*. 31 182.
- [6] Miller, J.S., Bethencourt, M.I., Hahn, M., Lee, T.R., West, J.L. (2006) Laser-scanning lithography (LSL) for the soft lithographic patterning of cell-adhesive self-assembled monolayers. *Biotechnology and bioengineering* 93 1060-1068.
- [7] Waugh, D.G., Toccaceli, C., Gillett, A., Ng, C.H., Hodgson, S., Lawrence, J. (2016) Surface treatments to modulate bioadhesion: A critical review. *Reviews of Adhesion and Adhesives* 4 69-103.
- [8] Mittal, K.L., Bahners, T. (2015) *Laser Surface Modification and Adhesion*. Beverly, MA, USA, Wiley-Scrivener.
- [9] Thakur, S., Neogi, S. (2015) Tailoring the adhesion of polymers using plasma for biomedical applications. *Reviews of Adhesion and Adhesives* 3 53-97.
- [10] Shukla, P., Waugh, D.G., Lawrence, J. (2016) Laser surface structuring of ceramics, metals and polymers for biological applications: A review, in: R. Vilar, L. Overend (eds) *Laser Surface Modification of Biomaterials: Techniques and Applications*. Oxford, UK, Elsevier Ltd.
- [11] Waugh, D.G., Lawrence, J. (2013) *Laser Surface Treatment of a Polymeric Biomaterial: Wettability Characteristics and Osteoblast Cell Response Modulation*. Philadelphia, PA, USA, Old City Publishing Inc..
- [12] Waugh, D.G., Lawrence, J., Brown, E.M. (2012) Osteoblast cell response to a CO<sub>2</sub> laser modified polymeric material. *Optics and Lasers in Engineering*. 50 236-247.
- [13] Ivanova, E.P., Hasan, J., Webb, H.K., Gervinskas, G., Juodkazis, S., Truong, V.K. (2013) Bactericidal activity of black silicon. *Nature Communications*. 4 1-7.
- [14] Chan, C.W., Hussian, I., Waugh, D.G., Lawrence J., Man, H.C. (2012) In vitro mesenchymal stem cell responses on laser-welded NiTi alloy. *Materials Science & Engineering C* 33 1344-1354.
- [15] Pflöging, W., Bruns, M. (2007) Laser-assisted modification of polystyrene surfaces for cell culture applications. *Applied Surface Science* 253 9177-9184.
- [16] Harnett, E.M., Alderman, J., Wood, T. (2007) The surface energy of various biomaterials coated with adhesion molecules used in cell culture. *Colloids and Surfaces B: Biointerfaces* 55 90-97.
- [17] Duncan, A.C., Weisbuch, F., Rouais, F., Lazare, S., Baquey, C. (2002) Laser microfabricated model surfaces for controlled cell growth. *Biosensors & bioelectronics* 17 413-426.
- [18] Yu, F., Mucklich, F., Li, P., Shen, H., Mathur, S., Lehr, C.M. (2005) In vitro cell response to a polymer surface micropatterned by laser interference lithography. *Biomacromolecules* 6 1160-1167.
- [19] Callewaert, K., Martelé, Y., Breban, L., Naessens, K., Vandaele, P., Baets, R. (2003) Excimer laser induced patterning of polymeric surfaces. *Applied Surface Science* 208-209 218-225.
- [20] Waugh, D.G., Lawrence, J. (2011) The enhancement of biomimetic apatite coatings by means of KrF excimer laser surface treatment of nylon 6,6. *Lasers in Engineering* 21 95-114.
- [21] Waugh, D.G., Lawrence, J. (2012) Modulating calcium phosphate formation using CO<sub>2</sub> laser engineering of a polymeric material. *Materials Science & Engineering C* 32 189-200.
- [22] MacGregor, K. (2010) The ageing population: U.K. focus for biomedical engineering - policy briefing. The Royal Academy of Engineering.
- [23] Taylor, W. (2009) *Technical Synopsis of Plasma Surface Treatments*. Institute of Packaging Professionals. Gainesville, FL, USA, University of Florida, p.12.
- [24] Lo, T.Y., Wang, Y.J., Liu, D.M., Whang, W.T. (2015) Surface characteristics and biofunctionality of a novel high-performance, hydrophilic Jeffamine-added fluoro-containing polyimide for biomedical applications, *Journal of Polymer Research* 22 12.
- [25] Biggs, M.J., Richards, R.G., Gadegaard, N., Wilkinson, C.D., Dalby, M.J. (2007) Regulation of implant surface cell adhesion: characterization and quantification of S-phase primary osteoblast adhesions on biomimetic nanoscale substrates. *Journal of Orthopaedic Research* 25 273-282.
- [26] Waugh, D.G., Lawrence, J., Morgan, D.J., Thomas, C.L. (2009) Interaction of CO<sub>2</sub> laser-modified nylon with osteoblast cells in relation to wettability. *Material Science and Engineering C* 29 2514-2524.
- [27] Waugh, D.G., Lawrence, J. (2011) On the use of CO<sub>2</sub> laser induced surface patterns to modify the wettability of poly(methyl methacrylate) (PMMA). *Optics and Lasers in Engineering* 48 707-715.
- [28] Waugh, D.G., Lawrence, J. (2011) Wettability and osteoblast cell response modulation through UV laser processing of nylon 6,6. *Applied Surface Science* 257 8798-8812.
- [29] Rance, D.G. (1982) Chapter 6 - thermodynamics of wetting: From its molecular basis to technological application, in D.M. Brewis (ed) *Surface Analysis and Pretreatment of Plastics and Metals*, UK, Applied Science Publishers.
- [30] Cefalas, A.C., Vassilopoulos, N., Sarantopoulou, E., Kollia, Z., Skordoulis, C. (2007) Mass spectroscopy

and ablation characteristics of nylon 6.6 in the ultraviolet. *Applied Physics A* 70 21-28.

[31] Steen, W.M., Watkins, K.G., Mazumder, J. (2010) *Laser Material Processing*, 4th Edition. UK, Springer.

[32] Waugh, D.G., Lawrence, J. (2015) *Laser Surface Engineering: Processes and Applications*. Cambridge, UK, Elsevier Ltd.

[33] Hao, L., Lawrence, J. (2005) *Laser Surface Treatment of Bio-Implant Materials*. New Jersey, USA, John Wiley & Sons Inc.

[34] Jung, Y.C., Bhushan, B. (2007) Wetting transition of water droplets on superhydrophobic patterned surfaces. *Scripta Materialia* 57 1057-1060.

### **Meet the Author**

Dr David Waugh joined the University of Chester as Programme Leader for Mechanical Engineering in May 2014 and is a founding member of the Laser Engineering and Manufacturing Research Group (LEMRC: [www.chesterlasers.org](http://www.chesterlasers.org)). Dr Waugh has published 2 books, 7 book chapters, 17 journal papers and 19 conference papers in laser material processing, healthcare engineering and wettability/adhesion characteristics. On account of Dr Waugh's wide ranging expertise he is a journal manuscript reviewer for 13 international journals and is an external expert for the European Union COST Action Research Programme.